A CONCENTRATION-DEPENDENT MODEL FOR SILVER COLLOIDS IN NANOSTRUCTURED SOL-GEL MATERIALS.

Jorge A. García-Macedo[1*], Alfredo Franco[1], Víctor Rentería[1], Guadalupe Valverde-Aguilar[2]

1. Instituto de Física, UNAM. Circuito exterior 04510. Ciudad Universitaria, Coyoacán. México D.F.
2. Department of Chemistry and Biochemistry, University of California, Los Angeles, CA 90095.

ABSTRACT

We report on the physical modelling of the photoconductive response of nanostructured sol-gel films in function of the silver nitrate concentration (ions and colloids). This model considers several factors as the silver nitrate concentration and the transport parameters obtained. The model is compared with others commonly used. 2d -hexagonal nanostructured sol-gel thin films were prepared by dip-coating method using a non-ionic diblock copolymer Brij58 (surfactant) to produce channels into the film. Silver colloids (metallic Ag^0 nanoparticles) were obtained by spontaneous reduction process of Ag^+ ions to Ag^0. These nanoparticles were deposited into the channels formed by the surfactant. The structure was identified by X-ray diffraction and TEM. An absorption band located at 430 nm was detected by optical absorption; it corresponds to the plasmon surface. Fit to this band with modified Gans theory is presented. Photoconductivity studies were performed on films with silver ions and films with silver colloids to characterized their mechanisms of charge transport in the darkness and under illumination at 420, 633 nm wavelengths. Transport parameters were calculated. The films with silver colloids exhibit a photovoltaic effect stronger than the films with silver ions. While, the last ones possesses a photoconductivity behaviour.

KEYWORDS: sol-gel, photoconductivity, silver colloids, surfactant.

1. INTRODUCTION

Optical properties of silver nanoparticles embedded in dielectric media are interesting because of their technological applications in photo electrodes for solar cells[1], optical switches[2] and electronic properties[3].

Nanoporous silica materials have been doped with metal nanoparticles to modify their properties and to obtain unique properties[4]. These materials have applications in nanotechnology as sensors, catalysts, etc.[5] Much effort has been devoted to prepare silver nanoparticles in both organic and inorganic materials. The use of inorganic oxide coatings rather than organic stabilizers provides several advantages[4]. The nanostructured sol-gel thin films prepared with poly(ethylene oxide)-based non-ionic diblock $[C_nH_{2n+1}(OCH_2CH_2)_yOH]$ copolymers, contain three distinct regions (figure 1): the framework that consists of silica or modified silica, the shell that is formed by the hydrophilic part of the surfactant (EO blocks which are water soluble) with residual solvent, and the core that is form by the hydrophobic part of the surfactant. We used a non-ionic diblock surfactant, Brij58 (($C_{16}H_{33}(OCH_2 CH_2)_{20}OH$), to create a long-ordered nanostructure in the thin films. The micelles possess a hydrophobic core surrounded by an outer shell of the EO blocks.

Nanostructured sol-gel thin films were doped with silver nitrate under acidic conditions. Photoconductivity studies under illumination and in the darkness were done in both thin films, with Ag^+ ions and metallic Ag^0 nanoparticles. The reduction of Ag^+ ions to silver colloids was detected by the typical sequence of color changes from colorless/white to black. The reduction process was monitored by UV-VIS absorption spectroscopy. A black silica thin films usually displays a plasmon band around 450 nm. In this paper, we report a theoretical model with concentration dependence to fit the conductivity on these films when ions or metallic particles are present.
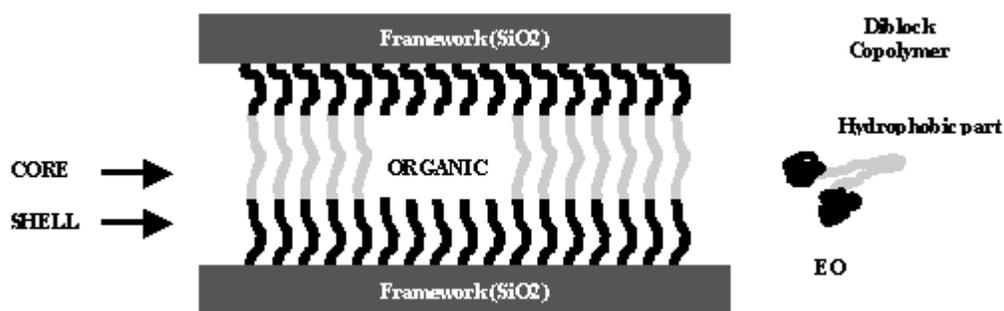
* Contact autor e-mail: gamaj@fisica.unam.mx

Figure 1. Sketch of the three regions of nanostructured sol-gel thin films prepared with diblock copolymers.

2. EXPERIMENTAL

Glass substrates were boiled in an acidic solution of sulphuric acid with hydrogen peroxide. Films were dip coated to the glass substrates at rate of 3.5 cm/min (see figure 2). The films were drawn with the equipment described previously that uses hydraulic motion to produce a steady and vibration-free withdrawal of the substrate from the sol[6]. Convection-free drying was critical to obtain high optical quality films.
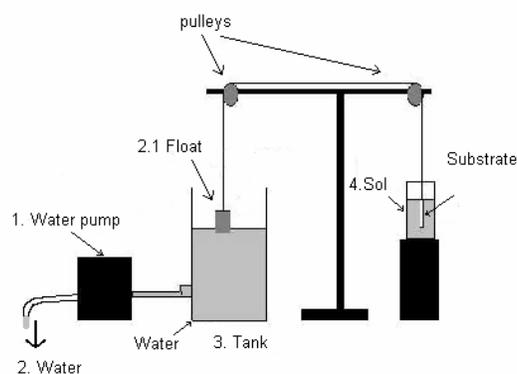

Figure 2. Experimental apparatus to prepare the mesostructured thin films by dip coating method.

All reagents were Aldrich grade. An initial solution was prepared with $AgNO_3$ (silver nitrate) dissolved in a small quantity of deionized water and nitric acid. Then was added 1 g of methanol, 5.4 g of TMOS (Tetra methyl orthosilicate), and 1.3-4 g of the neutral surfactant Brij58 ($C_{16}H_{33}PEO_{20}$). This initial solution was mixed and heated to 50-70 ºC for 20 minutes to homogenize the mixture. The final concentrations molar ratio were $AgNO_3$/ $C_{16}H_{33}PEO_{20}$ = 0.3-1.0.

The structure of the final films was characterized with X-ray diffraction (XRD) patterns. These patterns were recorded on a Siemens D500 diffractometer using Ni-filtered CuKα radiation with an integration time of 1 sec at low angle. Transmission electron microscopy (TEM) was taken with a JEOL 4000EX high-resolution TEM (HRTEM) at 400kV with 0.17 nm resolution.

For photoconductivity studies[7] silver electrodes were painted on the sample. It was maintained in a 10^{-5} Torr vacuum cryostat at room temperature in order to avoid humidity. For photocurrent measurements, the films were illuminated with light from an Oriel Xe lamp passed through a 0.25m Spex monochromator. Currents were measured with a 642 Keithley electrometer connected in series with the voltage power supply. The applied electrostatic field E was parallel to the film and perpendicular to the illumination. Light intensity was measured at the sample position with a Spectra Physics 404 power meter[7] (figure 3).
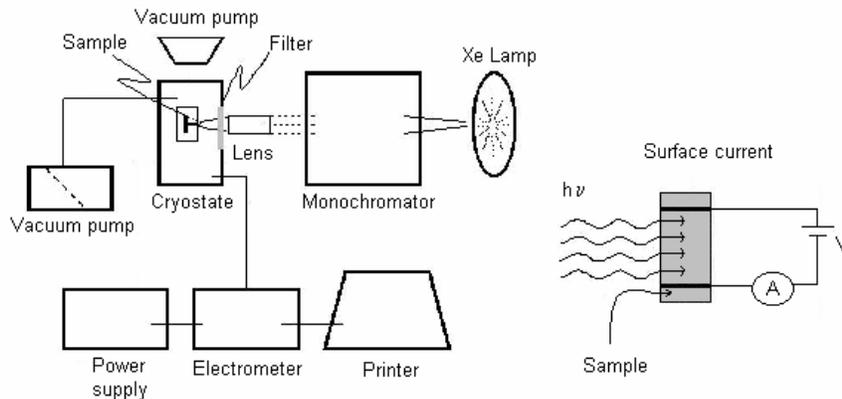
Figure 3. (a) Schematic diagram of the photoconductivity technique. Surface current was produced on the thin film when an electric field was applied it as it is shown in (b).

3. RESULTS

3.1 Crystalline

Samarskaya et al.[4] reported a lyotropic liquid crystalline phase of oligo (ethylene oxide) surfactants which house Ag^+ ions in the hydrophilic ethylene oxide head group and allow Ag^+ ions to distribute uniformly into the channels of mesoporous silica materials. We used the same recipe to prepare our films deposited on glass slides at different concentrations of AgNO3/Brij58 using the diblock copolymer Brij58 as template to form these channels. Figure 4 (a) shows the X-ray pattern from film with $AgNO_3$/Brij58 molar ratio equal to 0.7. The peak at $2\theta = 1.77°$, or a d-spacing of 50.0 Å, corresponds to the (100) peak of the 2d-hexagonal-phase structure. Transmission electron microscopy (TEM) was used to image films containing the silver colloids. The Figure 4 (b) shows the hexagonal array formed.
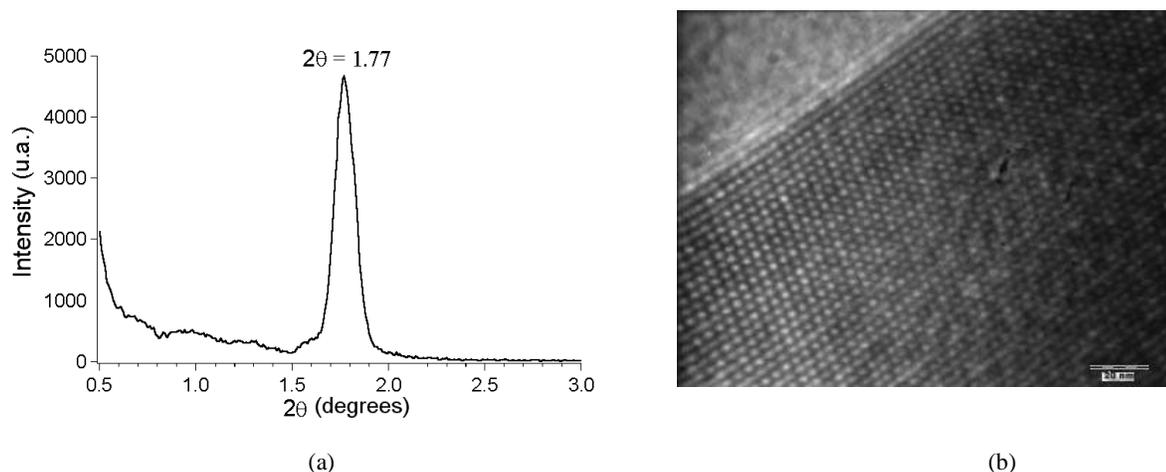

(a)

(b)

Figure 4. (a) X ray diffraction pattern for a sample with $AgNO_3$/Brij58 = 0.7 molar ratio. The (100) peak with $2\theta=1.77°$ corresponds to a 50.0 Å d-spacing. (b) TEM image from nanostructured sol-gel thin film with $AgNO_3$/Brij58 = 0.7 molar ratio, it shows the hexagonal array formed into the film using the diblock copolymer Brij58.

3.2 Optical absorption

Two kind of samples were studied, both with crystalline structure due to the employment of the diblock copolymer Brij58, but one of them possesses Ag^+ ions and the other possesses metallic Ag^0 nanoparticles. The existence of the metallic Ag^0 nanoparticles in the samples is evident from their optical absorption spectra. The films without metallic Ag^0 nanoparticles do not have the pronounced peak around 430 nm of those ones with the metallic nanoparticles. The position, height and width of the peaks change for every sample due to several factors: $AgNO_3$/Brij58 molar ratio, colloidal time formation and the possible Brij58 or silver oxide shell formation around colloids[8]. In figure 5 the optical absorption spectra for different $AgNO_3$/Brij58 molar ratios appear as well as their corresponding absorption coefficient at two different wavelengths: one is near to the region of the plasmon resonant frequency (420 nm) and the other one is out of that region (633 nm). It is noticeable that for the 0.5 relative concentration the optical absorption is larger than for any other relative concentration but it is due to the colloidal time evolution of the system in the film, even when the optical absorption spectra were measured at approximately the same time after the preparation of each one of the samples. However, the optical absorption value at 420 nm and at this time gives information about the nanoparticles concentration in each sample. This value surely changes with time and it would be interesting to follow the time dependence of the Ag^0 nanoparticles formation.
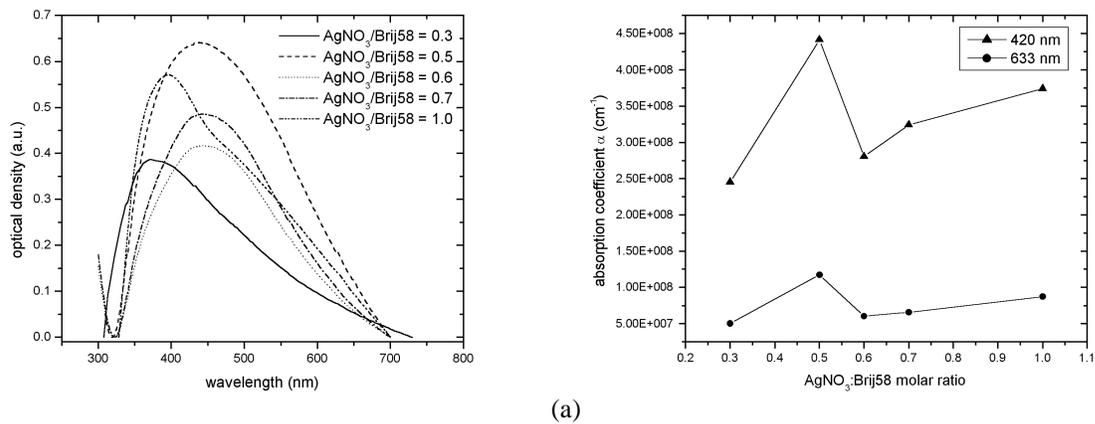

Fig 5. (a) Optical absorption spectra for different $AgNO_3$/Brij58 molar ratios. (b) Absorbance as function of $AgNO_3$/Brij58 molar ratio for two different illumination wavelengths: 420 nm (near to the plasmon peak) and 633 nm (any other).

The spectra shown in figure 5 exhibit asymmetry, suggesting they are formed by more than one resonance peak. Probably, one of those peaks is due to a copolymer shell formed around the nanoparticles[9]. The position of each peak is intimately related to the particles size distribution. Different $AgNO_3$/Brij58 molar ratios produce different sizes of the nanoparticles, even when all the samples were prepared under similar conditions[10]. Figure 6 shows a fit of the optical absorption spectrum corresponding to an $AgNO_3$/Brij58 molar ratio equal to 0.3. For the fitting it was employed a modified Gans model with two main peaks, one of them is related to the metallic silver particles and the other one is related to the nanoparticles with a copolymer shell around. In figure 6 *AR* is the nanoparticles axial ratio, *R* is the nanoparticles size, *n* is the medium refractive index, the continuous line is the spectrum shown in figure 5 (a), and the dashed lines are the two different peaks with their superposition, which practically reproduces the experimental spectrum.
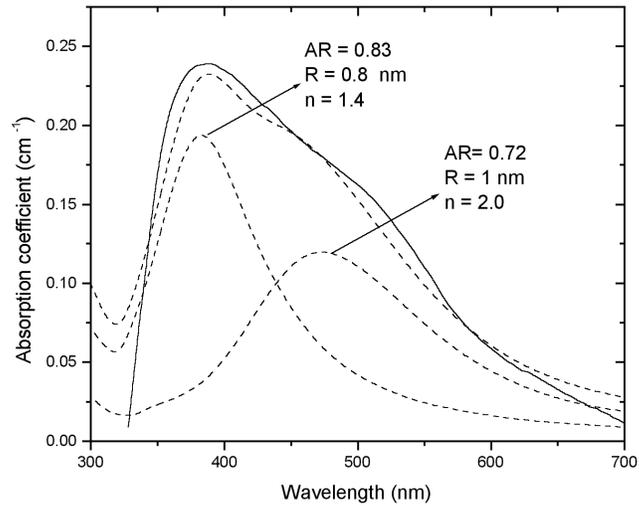
Fig 6. Gans fitting for the optical absorption spectrum of a sample with an $AgNO_3$/Brij58 molar ratio equal to 0.3 employing two main plasmon resonance peaks. The continuous line corresponds to the experimental results and dashed lines correspond to the fitting peaks and their superposition.

3.3 Dark conductivity

We compare the obtained values for dark conductivity at different relative concentrations $AgNO_3$ / Brij58 in the two kind of employed samples: with and without metallic Ag^0 nanoparticles. The dark conductivity experimental results for both kind of samples are shown in figure 7, in which it is easy to distinguish two different behaviors: for the samples with metallic Ag^0 nanoparticles the conductivity increases monotonically as the $AgNO_3$ / Brij58 molar ratio increases too, but for samples with Ag^+ ions the conductivity increases as the $AgNO_3$ / Brij58 molar ratio does until the conductivity reaches a saturation value at the larger concentrations measurements.

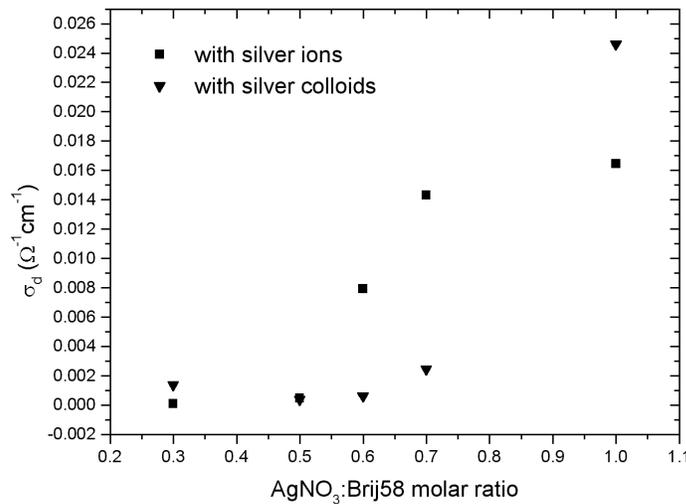Figure 7. Dark conductivity σ_d vs. $AgNO_3$ / Brij58 molar ratio.

Experimental results analysis begins with the Ohm's law expression:

$$\vec{J} = \sigma_d \, \vec{E} \, ,$$ (1)

but under the assumption of a current density $\vec{J}$ parallel to the applied electric field to the sample $\vec{E}$, the dark conductivity σ_d can be expressed as:

$$\sigma_d = qn\mu \, ,$$ (2)

where q is the charge of the charge carriers, n is the charge carriers density and μ is the mobility of the charge carriers in the material. This last relation indicates a linear dependence between the dark conductivity and the charge carriers concentration. If it is assumed a linear relation between the $AgNO_3$ / Brij58 molar ratio and the charge carriers concentration then figure 7 suggests a nonlinear dependence between the charge carriers mobility μ and the $AgNO_3$ / Brij58 molar ratio. This dependence has to be different for samples with and without metallic Ag^0 nanoparticles.

For samples with metallic Ag^0 nanoparticles the charge carriers mobility has to increase monotonically with respect to $AgNO_3$ / Brij58 molar ratio increments, and there are two main possible descriptions for this behavior: the first one is given by a power law, as is stated by percolation models for dielectric-metallic materials mixtures[11], the second one follows an exponential growth. Figure 8 shows both of the fits, employing the next equations:

$$\sigma_d(n) = qn\mu(n) = \begin{cases} qn\mu_0(n - n_c)^t \\ qn\mu_0 e^{An} \end{cases} ,$$

(3.a)

(3.b)

where the fitting parameters are t, A and the threshold concentration n_c .
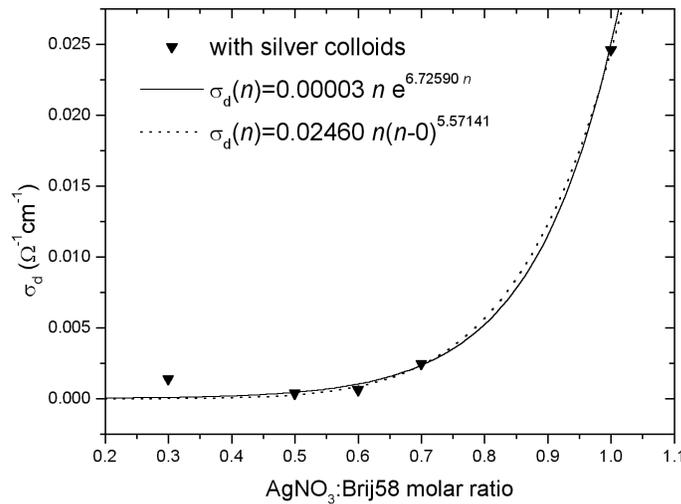

Figure 8. Best fits from dark conductivity vs. $AgNO_3$ / Brij58 molar ratio, for samples with metallic Ag^0 nanoparticles.

From the figure 8 it is not possible to discern about which is the best fit, but the values employed for the power law parameters (n_c=0, t=5.57141) are not usual in percolation theories, thus we will keep only the exponential description for the dark conductivity.

The conductivity in the samples with Ag$^+$ ions increases until it reaches a saturation value. We assume, for this kind of samples, the same exponential charge carriers mobility growth with respect to the AgNO$_3$ / Brij58 molar ratio at low molar ratios, but it is necessary to consider a mobility correction term due to the samples saturation behavior.

It is well known that in materials which exhibit ionic conductivity, their total current density is the result of two kinds of currents, each one with different physical origin: the first one is the usual ohmic behavior described by equation (1), but the second one is due to a diffusion process, in which ions are redistributed in the material by the applied electric field. This current of diffusion usually is described by Fick's law, i.e., is directly proportional to the gradient of the generated ions spatial distribution, and this current density oppose to the movement of the charge carriers in the direction of the applied electric field. Thus from any measurement of conductivity in this kind of materials it is obtained a conductivity value which is the result of two terms.

We do not work directly with this two terms, instead we propose equation (4), which gives the conductivity rate of change with respect to the ions concentration.

$$\frac{d\sigma_d(n)}{dn} = A\,\sigma(n) + \frac{\sigma(n)}{n} - B\sigma(n)^2 \,, \tag{4}$$

The third term in equation (4) is intimately related to the ionic diffusion process, giving place to an apparent saturation value for the conductivity. If the constant B were equal to zero then there would not be diffusion term and the equation would recover the expression (3.b), with n a charge carriers concentration proportional to the AgNO$_3$ / Brij58 molar ratio.

From equation (4), the ionic conductivity is given by

$$\sigma_{di}(n) = \frac{A^2 e^{An}n}{ABe^{An}n - Be^{An} + C} \,, \tag{5}$$

where C is an arbitrary constant, and the subscript i is employed here to distinguish the ionic conductivity ($B \neq 0$).

Figure 9 shows the fitting curve of the experimental data for the samples with silver ions, employing equation (5). It is interesting to note in the inset that the conductivity tends to an asymptotic value for large silver concentration, but just before that asymptotic value the conductivity reaches a maximum value, just where there is a vertical dashed line in the inset.

If the samples follow the behavior given by equation (5) it would be possible to know the current density of diffusion and also to know the spatial ionic distribution in the sample. To know if this behavior is adequate for these samples it would be convenient to measure the tiny descendent part in the inset graphic at large AgNO$_3$/Brij58 molar ratios.

Thus dark conductivity is well described by an exponential growth for the two kinds of samples, but for the ionic ones the conductivity reaches an asymptotic value due to an ionic spatial redistribution. The exponential growth does not correspond to a similar growth in the charge carriers concentration, but it does to a similar growth in the mobility, which means that the AgNO$_3$/Brij58 molar ratio changes the samples physical conditions, maybe the changes are in the atomic potentials of the Brij58 surfactant and of the SiO$_2$ net structure. It is also interesting to see in figure 7 the next fact: ionic conductivity grows faster in ionic samples than in colloidal ones, maybe because every Ag$^+$ ion contributes to the current density in the ionic films but in the films with metallic Ag^0 nanoparticles the probability that all the nanoparticles contributes with at least one conduction electron to the system is very low.
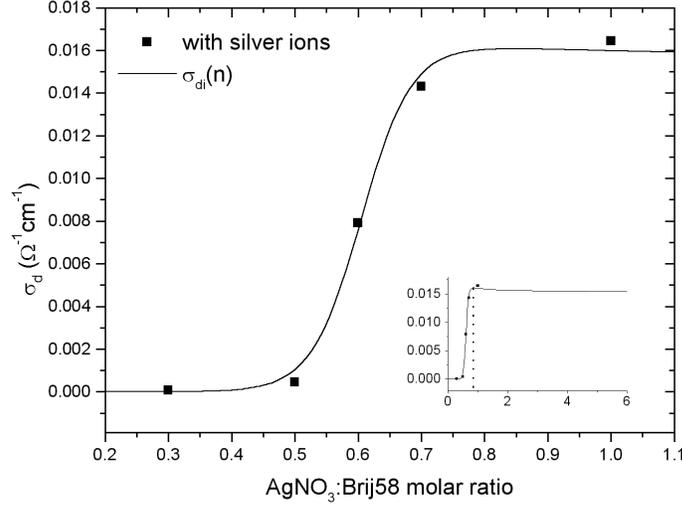
Figure 9. Dark conductivity vs. Relative $AgNO_3$ / Brij58 concentration for the samples with silver ions. The continuous line is the best fit employing equation (5) with the next parameter values: A=23.58984, B=1540.80440, C=3.34x10^{10}. The inset has the same units than the main graph, but its horizontal axis is enlarged to show the existence of a maximum value for conductivity at the concentration indicated by the dashed vertical line.

3.4 Photoconductivity

The conductivity under illumination exhibits the same qualitative behavior than the dark conductivity does for both kind of samples: with and without silver colloids, as one can distinguish from figure 10.

Usually[7] Ohm's law under light illumination is given by

$$\vec{J} = \vec{J}_{ph} + \left(\sigma_d + \sigma_{ph}\right)\vec{E} \, , \tag{6}$$

with $\vec{J}_{ph}$ a photovoltaic current density, and σ_{ph} the photoconductivity. When the current densities are assumed to be parallel to the electric field $\vec{E}$ equation (6) becomes into the next one:

$$J = \frac{q\phi l_0 \alpha I}{h\nu} + \left(\sigma_d + \frac{q\phi\mu\tau\alpha I}{h\nu}\right)E \, , \tag{7}$$

with ϕ as the quantum yield of charge carrier photogeneration, l_0 as the charge carrier mean free path, α as the sample absorption coefficient, I as the light intensity at the frequency ν of illumination, h as the Planck´s constant, and τ as the charge carriers mean lifetime.

The sample absorption coefficient α depends on the silver nanoparticle concentration, the same situation occurs, as we have seen yet, with the charge carriers mobility.

It is possible to incorporate in equation (7) the dependence of the charge carriers mobility with the charge carriers concentration. If this equation describes a material with only metallic Ag^0 nanoparticles then all its terms have to correspond to an electronic conductivity in nature, but if this equation describes a material with silver ions then equation (7) has two different kind of terms: one of them is merely ionic in nature and the other one, the photoconductivity, has an electronic origin.

In the case of a sample with metallic Ag^0 nanoparticles, equation (7) becomes into:

$$J = \frac{q\phi l_0 \alpha I}{h\nu} + qn\mu_0 e^{An} E + q\frac{(\phi\tau - \phi_s\tau_s)\alpha I}{h\nu}\mu_0 e^{An} E, \tag{8}$$

where the first term is the photovoltaic one, the second term corresponds to the dark conductivity, and the third term is the photoconductivity. In this last term we empirically include the factors $\phi_s\tau_s$ in order to represent a plasmon scattering process, which is evident when the samples are illuminated at the plasmon resonant frequency. In figure 10 it is clear that the conductivity under the plasmon resonant frequency illumination is less than that one under an illumination with a wavelength out of the resonant peak (633 nm wavelength).

In the case of a sample with silver ions, equation (7) becomes into:

$$J = \frac{q\phi l_0 \alpha I}{h\nu} + qn\mu_0 \frac{Ce^{An}}{ABe^{An}n - Be^{An} + C}E + q\frac{\phi\tau\alpha I}{h\nu}\mu_0 e^{A'n}E, \tag{9}$$

where the first term is the photovoltaic one, the second term corresponds to the dark conductivity, and the third term is the photoconductivity, which is electronic in nature and, in consequence, charge carriers mobility is like that of equation (8), with its own growth constant A'. In equation (9) there is not plasmon scattering term, because silver ions do not have silver plasmons. In figure 10 it is clear that ionic samples never decreases their conductivity due to illumination.

The second term of equation (9) is obtained from equation (5) and making use of the fact that equation (5), with $B=0$, recovers equation (3.b) only if the next relation is hold:

$$\frac{A^2}{C} = q\mu_0. \tag{10}$$

Figure 10 shows the experimental results for both kind of samples and their best fittings employing equations (9) and (10). It is noticeable that ionic conductivities under illumination are not zero at zero silver concentration, but it is due to a lack of information about the exact relation between the sample absorption coefficient α dependence and the silver concentration. At zero concentration α would be zero and, in consequence, continuous lines in figure 10 would reach zero conductivity. There is another interesting feature, for larger silver ionic concentrations equation (9) predicts a constant increase in the conductivity under illumination, which is opposite to the expected dark conductivity behavior depicted by equation (5).
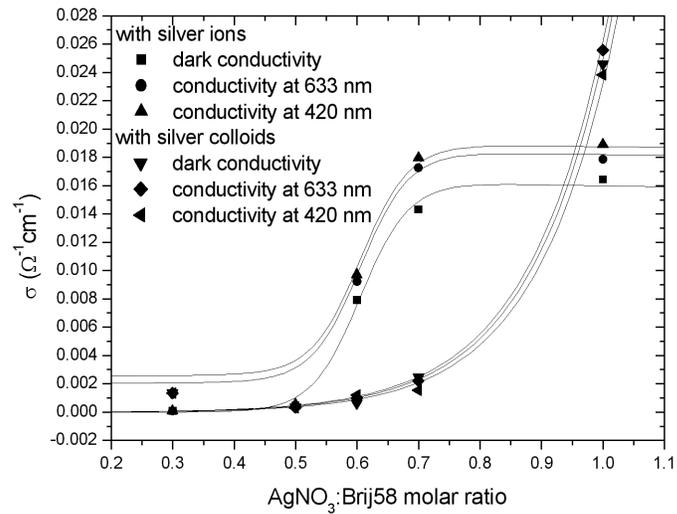
Figure 10. Plot of the conductivity vs. AgNO₃/Brij58 molar ratio. Continuous lines are the experimental fitting results employing equations (8) and (9). The employed parameters are contained in table I.

σ	With silver colloids			With silver ions		
	Dark	633 nm	420 nm	Dark	633 nm	420 nm
$q\mu_0$ [cm^2/Ω]	0.00003	0.00003	0.00003	-----	-----	-----
A [cm^3]	6.72590	6.72590	6.72590	23.58984	23.58984	23.58984
$q\dfrac{\phi\tau\alpha I}{h\nu}\mu_0$ [Ω^{-1}cm^{-1}]	0	0.05	0.05	0	0.0020	0.0025
$q\dfrac{\phi_s\tau_s\alpha I}{h\nu}\mu_0$ [Ω^{-1}cm^{-1}]	0	0	0.12	-----	-----	-----
B [cm^4 Ω]	-----	-----	-----	1540.80440	1540.80440	1540.80440
C [cm^4 Ω]	-----	-----	-----	3.34×10^{10}	3.34×10^{10}	3.34×10^{10}
A' [cm^3]	-----	-----	-----	-----	0.1	0.1

Table I. Employed value parameters for conductivity fittings.

4. CONCLUSIONS

Films with Ag$^+$ ions were prepared by sol-gel method. The films exhibit a hexagonal crystalline structure. Ag^0 metallic nanoparticles were obtained after spontaneous reduction of the Ag$^+$ ions. Photoconductivity measurements were carried on both kinds of films as function of the AgNO₃/Brij58 molar ratio. The experimental results shown a different behavior for each kind of film. Films with Ag$^+$ ions exhibit a saturation conductivity value. Films with Ag^0 metallic nanoparticles exhibit an exponential growing conductivity. The experimental results were fitted satisfactorily with a mobility concentration dependent model.

5. ACKNOWLEDGMENTS

6. REFERENCES

1. H. Kozuka, "Metal nanoparticles in gel-derived oxide coating films: control and application of surface plasma resonance". *SPIE* **3136**, 304 (1997).

2. C. Weiping, T. Ming, Z. Lide. "Characterization and the optical switching phenomenon of porous silica dispersed with silver nano-particles within its pores*". J. Phys: Condens. Matter*. **8**, L591 (1996).

3. Y. Masumoto, T. Kawamura. "Biexciton lasing in CuCl quantum dots". *Appl. Phys. Lett.* **62**(3), 225-227 (1993).

4. O. Samarskaya, O. Dag. "Silver Nitrate/Oligo(ethylene Oxide) Surfactant/Mesoporous Silica Nanocomposite Films and Monoliths". *J. Colloid and Interf. Sci.* **238**, 203-207 (2001).

5. H. Winkler, a. Birkner, V. Hagen, I. Wolf, R. Schmechel, H. Seggern, R. A. Fischer. "Quantum-confined gallium nitride in MCM-41". *Adv. Mater.* **11**, 1444-1448 (1999).

6. F. Nishida, et al. " In situ fluorescence probing of the chemical changes during sol-gel thin film formation". *J Am. Cer. Soc.*, **78**, 1640-1648 (1995).

7. J. García M., A. Mondragón, J. M. Hernández, J. L. Maldonado R. "Photocurrent determination of charge transport parameters in $KNbO_3:Fe^{3+}$". *Opt. Mat.* **3**, 61 (1994).

8. Luis M. Liz-Marzán, Michael Giersig, and Paul Mulvaney. "Synthesis of nanosized gold-silica core-shell particles". *Langmuir.* **12**, 4329-4335 (1996).

9. A. Campton, P. Kambhampati. "Surface-enhanced Raman Scattering". *Chemical Society Reviews* **27**, 241-250 (1998).

10. Wiping Cai, H. Hofmeister, T. Rainer. "Surface effect on the size evolution of surface plasmon resonances of Ag and Au nanoparticles dispersed within mesoporous silica". *Physica E* **11**, 339-344 (2001).

11. D. Toker, D. Azulay, N. Shimoni, I. Balberg, and O. Millo. "Tunneling and percolation in metal-insulator composite materials". *Phys. Rev. B* **68**, 041403 (2003).